

DETERMINATION OF MINORITY CARRIER DIFFUSION LENGTHS IN SILICON SOLAR CELLS FROM PHOTOLUMINESCENCE IMAGES

J.Giesecke¹, M.Kasemann², M.C.Schubert², B.Michl³, M.The¹, W.Warta¹, P.Würfel⁴

¹ Fraunhofer Institute for Solar Energy Systems (ISE), Heidenhofstr. 2, 79110 Freiburg, Germany

² University of Freiburg, Materials Research Center, Stefan-Meier-Str. 21, 79104 Freiburg, Germany

³ Schott Solar GmbH, Carl-Zeiss-Str. 4, 63755 Alzenau, Germany

⁴ Institute for Applied Physics, University of Karlsruhe, 76128 Karlsruhe, Germany

¹ phone: +49 761 4588 5631, fax: +49 761 4588 9250, email: johannes.giesecke@ise.fraunhofer.de

ABSTRACT: Lately a new luminescence based spatially resolved method to measure minority carrier diffusion lengths on Silicon Solar cells was introduced using Electroluminescence (EL) [1]. The idea of this method is to analyze the reabsorption-shaped form of the emitted luminescence spectrum with optical filters, enabling one to determine the depth distribution of excess minority carriers which is directly related to diffusion length. This article is concerned with the extension of this method to Photoluminescence (PL), allowing for a diffusion length mapping in all stages of cell production. Problems associated with this method - such as filter inhomogeneities, fluorescence of filters, texturing, the nature of surface reflection and surface recombination - are addressed. Different PL measurement setups are discussed theoretically and with respect to measurement results. Diffusion length images measured with the technique are demonstrated.

Keywords: diffusion length / lifetime, photoluminescence, silicon

1 INTRODUCTION

Spatially resolved lifetime mapping is nowadays vitally important in distinguishing between different causes to the deficiency of devices.

For spatially resolved diffusion length maps of solar cells, one has long been restricted to Spectrally Resolved Light Beam Induced Current (SR-LBIC) [2], which has the disadvantage of very long measuring times due to a scanning process. In addition, the separation of surface recombination and bulk diffusion length is associated with too much uncertainty, providing a further stimulus to push the development of imaging techniques that have the potential to be able to separate these two terms thoroughly.

Measuring lifetimes of wafers can be done by Microwave Photoconductance Decay (μ -PCD) [3], which involves a time consuming scanning process as well, by Quasi Steady State Photoconductance (QSSPC) [4], which is actually a global method of lifetime determination, and by Carrier Density Imaging (CDI) [5], which measures lifetimes using the absorption or emission of black body radiation by excess carriers.

Photoluminescence Imaging as a fast alternative to scanning methods has been applied to determine diffusion lengths as well [6,7], the problems associated with obtaining absolute values are addressed in detail in [6].

Subject of this work is the application of PL Imaging to diffusion length determination according to an approach introduced by Würfel et al [1]. This approach, which will be referred to as 'Luminescence Intensity Ratios (LIR)' in the following, is equally compatible with EL and PL conditions. It is based on the spectral analysis of the luminescence spectrum emitted from the surface of a sample. Due to reabsorption within the sample, the shape of the emitted luminescence spectrum depends on the generation depth of luminescence radiation in the sample and thus on the shape of the

excess minority carrier distribution. Deep generation will shift the emitted spectrum to lower photon energies, since higher photon energies are more likely to be reabsorbed. Appropriate injection of excess charge carriers near the front surface of a sample will therefore allow for a determination of the depth profile of emission which is linked to the depth profile of excess carrier density, which in turn decays with a bulk diffusion length L . The spatially resolved analysis of the emitted luminescence spectrum is done by the division of sample images taken with a CCD-camera with different optical short pass filters at appropriate edge-wavelengths.

2 THEORY

In EL as well as PL imaging, the electronic system of a silicon sample is driven into an excited state from which it relaxes back to equilibrium via recombination. With a constant excitation (EL: applied forward bias, PL: laser excitation) the sample will reach an excited steady state. The excess charge carrier density depth distribution $\Delta n(z)$ can then be calculated as the solution to a second order boundary value problem based on Fick's first law of diffusion and the continuity equation.

$$-D_e \partial_z^2 \Delta n(z) + \frac{\Delta n(z)}{\tau} = G \quad (1)$$

with the diffusion constant D_e (p-type base), the minority carrier lifetime τ and the generation rate G . Solutions $\Delta n(z)$ depend on the given boundary conditions. In the case of EL the boundary value problem is homogeneous ($G=0$) and excitation comes in via the boundary condition of an applied forward bias at the pn-junction, whereas in the case of PL on wafers, excitation comes in via an inhomogeneity $G(z)$, while boundary conditions are determined by surface recombination velocities only.

The solution $\Delta n(z)$ is linked to the quasi-fermi-level-splitting $\Delta \eta$, a quantity describing the deviation from equilibrium in terms of a chemical potential, which itself

enters in the generation rate of photons per volume and energy increment as follows

$$g_\gamma(E_\gamma, z) = \frac{\alpha(E_\gamma)E_\gamma^2}{4\pi^2\hbar^3c^2 \left(\exp\left(\frac{E_\gamma - \Delta\eta(z)}{k_B T}\right) - 1 \right)} \quad (2)$$

This is otherwise referred to as generalized Planck law of radiation [1,8,9,10]. E_γ denotes the Energy of a generated photon and $\alpha(E_\gamma)$ denotes the band to band absorption coefficient of silicon at this very energy.

A proportion of the photons generated this way is partly being reabsorbed on its way out of the sample. The rate of photons reaching the surface per area and energy increment G_γ becomes

$$G_\gamma(E_\gamma) = (1 - r_f(E_\gamma)) \int_0^d \exp(-\alpha(E_\gamma)z) g_\gamma(E_\gamma, z) dz \quad (3)$$

Here, r_f denotes the frontside reflectivity of the sample. For simplicity reasons, only direct emission is considered in eq. (3), in fact three additional orders of reflection have been considered in the simulations underlying our measurement evaluations. The first of these, being a simple reflection at the back surface of the sample, is seen as indispensable.

Using optical shortpass filters for the acquisition of sample images with a CCD-camera, the detected camera signal in pixel j , $\Phi_{cam}(\lambda, j)$ can be described as

$$\Phi_{cam}(\lambda, j) = \int_0^\infty dE_\gamma G_\gamma(E_\gamma, j) QE_{cam}(E_\gamma) T_{sp,\lambda}(E_\gamma) \quad (4)$$

with the quantum efficiency QE_{cam} of the CCD-camera and the transmission curve $T_{sp,\lambda}$ of a short pass optical filter with an edge wavelength of λ .

The luminescence intensity ratio $R = \Phi_{cam}(\lambda_1, i) / \Phi_{cam}(\lambda_2, i)$ is sensitive to bulk diffusion length $R = R(L)$, as the following figure illustrates.

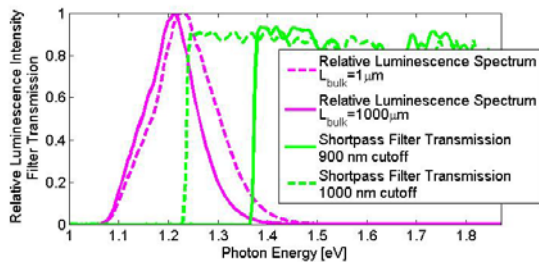


Figure 1: Typical spectrum of luminescence emitted from the surface of a solar cell. The simulation of these spectra is based on an EL forward bias of 630 mV, a sample thickness of 250 μm and a SiN-Antireflection coating. Note that the spectrum is already weighted by the quantum efficiency of the detecting CCD-camera.

The above figure provides a good illustration of the diffusion length dependence of intensity ratios of images taken with different optical filters. In this setup, large diffusion lengths yield higher intensity ratios than small ones, which would not occur if there was no reabsorption.

The good contrast at low diffusion lengths deteriorates towards higher ones, revealing a problem in bulk diffusion length determination when uncertainty of back surface recombination S_b is high, but at the same time offering an efficient mapping tool for S_b at well

known very high diffusion lengths [1] (for instance in FZ-material).

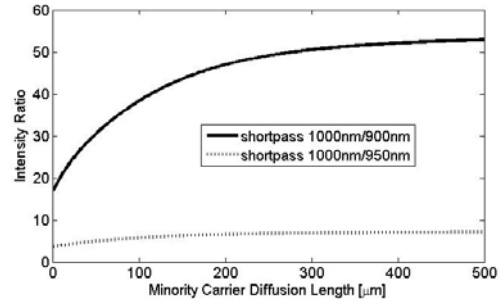


Figure 2: The intensity ratio of light intensities detected with different shortpass filters is plotted against the electron diffusion length in a p-doped base material.

3 EXPERIMENTAL SETUP

A conventional PL setup consists of a laser that excites excess charge carriers in a sample, allowing for detection of radiative recombination of these charge carriers with a CCD-camera on the same side as generation takes place (necessary for metallized samples). Here, in addition, a back-illuminated setup is introduced. The first setup requires the use of strong optical long pass filters in order to suppress detection of laser light within the camera, while the latter uses the sample itself as a longpass filter of laser radiation.

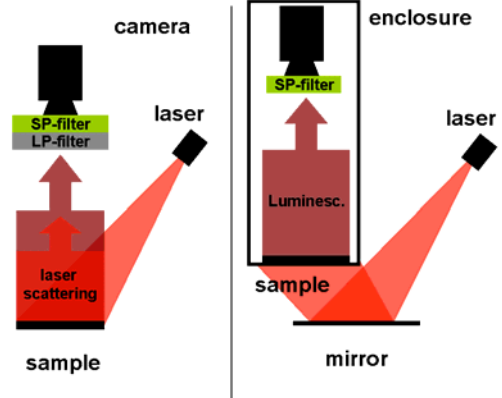


Figure 3: Illustration of the two experimental setups. The front-illuminated setup (left) requires a strong suppression of reflected laser light via a long pass optical filter, whereas the back-illuminated setup (right) uses the sample itself as a much stronger filter of laser light. However, PL-imaging on metallized devices is restricted to front-illumination.

Our calculations suggest that a sufficient suppression of stray light from the exciting laser must be stronger than 9 orders of magnitude. This relates to carrier densities corresponding to a very poor diffusion length of less than 5 μm at a sample reflectivity of 15% and isotropic scattering of reflected light [17].

At an exciting wavelength of 790 nm, the absorption length of silicon is of the order of 10 μm , leading to a suppression of laser light of more than 10 orders of magnitude over a typical wafer thickness of 260 μm . This suppression is stronger than any single longpass filter can guarantee. In addition, the mandatory use of one or even

two longpass filters in the first setup implies new artefacts such as reflections between the filters or fluorescence of semiconductor nano-crystallites (which are used to sharpen the transmission edge in such filters) [11]. As will be seen, the precision requirements of the LIR-method are too demanding to be able to tolerate such artefacts.

4 OBSTACLES ON THE WAY TO DIFFUSION LENGTHS

Several obstacles had to be overcome before it was possible to generate reliable diffusion length images of devices with the LIR-method:

It turned out that the quantum efficiency curve $QE_{cam}(E_\gamma)$ provided by the manufacturer was wrong. A relative quantum efficiency curve had to be measured at several chip temperatures.

Another problem was the influence of back surface reflectivity r_b on intensity ratios $R(L)$. Only global values for r_b rather than spectrally resolved ones were available. The directionality of back surface reflectivity may also contribute to a systematic error in diffusion length imaging [12]. This problem has been solved by a calculation of back surface reflectivity from the shape of front side reflectivity-curves near the silicon bandgap. With a linear extrapolation of the front side reflectivity and the spectral absorption of bulk silicon between front and backside, information on r_b is obtainable.

The influence of temperature on intensity ratios $R(L)$ must not be neglected. This is particularly important if the sample is not cooled to a well defined temperature, since especially in PL-imaging, temperatures of around 312 K are typical at an equivalent of one sun illumination. But even in EL, temperatures of around 307 K have been measured at current densities of about 40 mA/cm² if the sample was mounted only via electrical contact pins.

Texturing of devices is an issue that leads, uncorrected, to a systematic overestimation of diffusion length according to the LIR-method. This can be explained by the fact, that a textured sample surface usually has a higher point spread than a plane sample [13,14,15], which implies a higher proportion of detected photons that are emitted with an inclination towards the sample surface normal. These photons usually have to pass a longer way within the sample, so due to reabsorption the emitted luminescence from a sample surface with a high point spread is shifted to lower energies, leading to a higher intensity ratio than in the case of a zero point spread. This is experimentally confirmed by the following diffusion length measurement on a random pyramid textured solar cell.

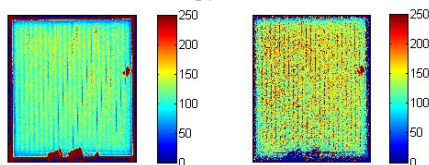


Figure 4: Diffusion length images [μm]. EL image (left) of a 2x2cm random pyramid textured cell, yielding a mean bulk diffusion length of $133\pm 2\mu\text{m}$ the corresponding PL image (right) yields a mean bulk diffusion length of $140\pm 4\mu\text{m}$. A global QE-measurement

yields an effective diffusion length ¹ $L_{eff}=88\mu\text{m}$ corresponding to $L_{bulk}=92\mu\text{m}$ at a thickness of $326\mu\text{m}$ and a back surface recombination velocity of $S_{back}=110\text{cm/s}$ [16]. EL and PL values are astonishingly close at a much higher level than the reference measurement. This is a confirmation of the above consideration that a rough surface leads to a shift of emitted luminescence to lower photon energies, resulting in an overestimation of bulk diffusion length.

One severe problem in determining diffusion lengths with the LIR-method were laterally inhomogeneous short pass filters. Spatially resolved transmission measurements over the whole surface of all used short pass filters strongly suggest that this inhomogeneity is caused by a variation of edge-wavelength due to a variation of the thickness of deposited dielectric layers on filters. This variation may be as small as 1nm but it may also easily exceed 10nm, which implies dramatic consequences for the diffusion length determination via intensity ratios.

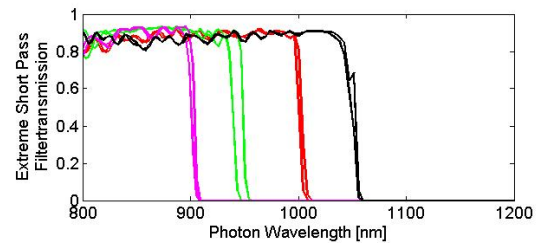


Figure 5: These transmission curves reveal the maximum span of edge-wavelength of filters measured over the whole filter area. Filters are specified at edge wavelengths of 900, 950, 1000 and 1050 nm. In the case of the 950 nm short pass, the edge wavelength spans over a range of more than 10 nm.

A possible solution to this lies in acquiring n images with each filter and turning the filter by an angle of $360^\circ/n$ from one image to the next as proposed in [1]. Taking the mean value of all images corresponding to one filter should reduce the problem, however this solution is not satisfying in every respect, since it is neither clear which transmission curve is to be taken in order to compute the intensity ratio curve $R(L)$, nor is there a maximum overlap of each surface element of the filter with each CCD-pixel. Furthermore, turning filters leads to an additional blurring of images because of a non-planar filter surface. Since it seems harder than previously assumed to find adequate filters that meet the high homogeneity requirements, a new approach was found in order to handle this problem:

In this approach, the filter surface is divided into a symmetric pattern of sections, in each of which the transmission curve is assumed to be constant. Spectral filter transmission is measured in the center of each section i to any pixel j on the CCD-chip at a given aperture is determined in weight functions W_{ij} . This approach led to convincingly converging diffusion length maps for different filter combinations and to a good agreement with other measurement methods.

¹ Note, that in the evaluation of the QE-curve the oblique entrance of the generation light at the textured surface is accounted for.

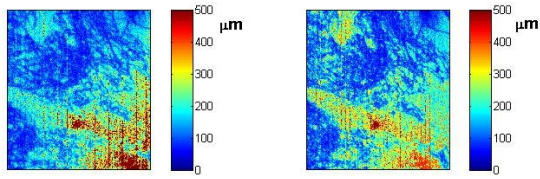


Figure 6: Diffusion length images in μm of a multicrystalline solar cell from a combination of 1000nm/950nm short pass filters (EL). Neglecting filter inhomogeneities (left) leads to a strong drift in the diffusion length map, taking these inhomogeneities into account completely removes the drift and leads to a better agreement with results from other filter combinations.

Details concerning this correction technique will be presented more elaborately in a forthcoming publication.

5 DIFFUSION LENGTH IMAGES FROM ELECTROLUMINESCENCE

Applying the above mentioned correction technique, EL diffusion length maps according to the LIR-method were in good agreement with both SR-LBIC maps and a global QE-measurement.

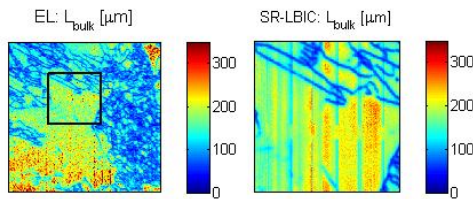


Figure 7: Comparison of an EL diffusion length map to an SR-LBIC map. EL diffusion lengths are calculated from a filter combination 1000nm/900nm. The SR-LBIC image shown represents a section of the EL-image as indicated (left).

SR-LBIC calculates effective diffusion lengths that were converted to bulk diffusion lengths at a given bulk thickness and back surface recombination S_b . The cell shown in fig. 7 has a screen-printed Al back surface field with $S_b \approx 750\text{cm/s}$ [16]. The bulk diffusion length values calculated on this basis from the SR-LBIC map agree well with the EL result. Both EL and SR-LBIC are in good agreement with a globally (QE) determined bulk diffusion length of $L_{\text{bulk}} = 233\mu\text{m}$ in the center quarter of the SR-LBIC map shown.

6 DIFFUSION LENGTH IMAGES FROM PHOTOLUMINESCENCE ON WAFERS

6.1 Front-illumination

From intensity ratios measured with the front-illuminated PL-setup at present reliable diffusion length maps cannot be obtained. Generally, intensity ratios are too low in order to yield diffusion lengths comparable to other measurement methods. One might expect this to be caused by an offset on each image due to laser reflection. This offset reduces intensity ratios to where corresponding diffusion lengths are underestimated. But an estimate of the amount of laser light passing the

respective long pass filters [17] suggests that this cannot be due to laser light. The implied offset must stem from another effect, which we suspect to be an effect of fluorescence of the applied long pass absorption filters. The existence of such an effect has clearly been shown from experiments conducted in our PL-laboratory. Further investigations on this topic are ongoing.

6.2 Back-illumination

In the back-illuminated setup, the calculation of diffusion lengths from intensity ratios has to be modified at one point. The rate of luminescence radiation reaching the backsurface of a sample is ²

$$G_y(E_y) \propto \int_0^d \exp(-\alpha(E_y) \cdot (d-z)) g_y(E_y, z) dz \quad (5)$$

This leads to a completely different shape of the calibration curve $R(L)$.

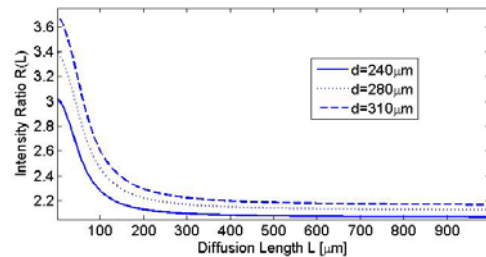


Figure 8: Intensity ratios obtained with back-illumination. The dependence on sample thickness is particularly critical in high lifetime areas.

This modification involves one disadvantage in the determination of diffusion lengths, being that there is a very strong dependence of intensity ratios on sample thickness d . In well passivated material at lifetimes of the order of $100\mu\text{s}$, this may imply

$$\left| \frac{\partial R(L, d)}{\partial d} \right| \gg \left| \frac{\partial R(L, d)}{\partial L} \right| \quad (6)$$

leaving no way around a thorough mapping of thickness.

In this work, d has been measured on many spots of a sample in order to achieve a pixelwise thickness-map by interpolation. Thickness variations coincide with variations of intensity ratios. Diffusion length was calculated at each pixel taking into account the local sample thickness. The resulting map still contains several areas where interpretation in terms of diffusion length is not possible because of intensity ratios below the range of $R(L)$. Interestingly, the pattern of these areas correlated well with a pattern of too low intensity ratios due to filter inhomogeneities.

Comparing this diffusion length map to a conventionally acquired one (μ -PCD), a slight systematic underestimation of diffusion lengths with the LIR-method can be noticed. However, facing the adverse measuring conditions caused by the very low contrast $\partial R(L)/\partial L$ the obtained result is astonishingly close to reference measurements. Taking account of filter inhomogeneities leads to the following image.

The remaining deviation from diffusion length maps acquired with established methods can have several causes, being either an insufficient thickness

² Note the difference between eqn. 3 and eqn. 5.

measurement, an insufficient measurement preparation to the correction of filter inhomogeneities, a remaining proportion of laser light passing the sample in very thin regions or even a point spread due to surface roughness.

In low cost material characterization as the possible area of application though, this will not be severe since contrast is good for $L_{bulk} < 200\mu\text{m}$.

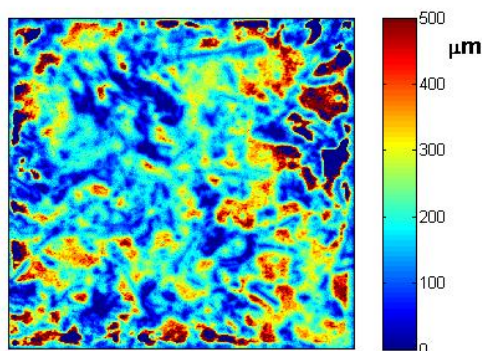


Figure 9: This diffusion length map considers both thickness variations and filter inhomogeneities. It is based on image acquisition time of 3 s. A reduction to 1 s should be possible. In some areas interpretation in terms of diffusion length is not possible, because intensity ratios are below the range of $R(L)$.

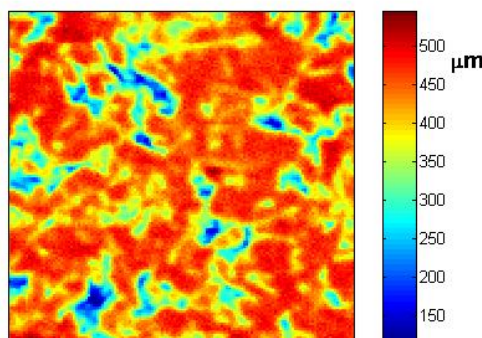


Figure 10: μ -PCD lifetime map converted to diffusion lengths which are significantly higher in this image than in a PL intensity ratio map.

7 CONCLUSION

It is possible to determine minority carrier diffusion lengths from intensity ratios of photoluminescence images of wafers acquired with different short pass optical filters. In this work a back-illuminated setup was found to be more suitable to this measurement method than the conventional front-illuminated PL-setup, which is most likely due to a fluorescence of long pass optical absorption filters used to prevent laser light from being detected in the camera.

The remaining drawbacks in diffusion length determination according to the LIR-method are the distinction between bulk and surface recombination, the mentioned problems associated with texturing and an ambiguity in absorption data given in [18-22].

8 ACKNOWLEDGEMENTS

This work was funded by the German Federal Ministry of Environment, Nature Conservation and Nuclear Safety under contract number 0327616 (PVQC).

The authors would like to thank E.Schäffer for conducting SR-LBIC and SR-measurements.

9 REFERENCES

- [1] Würfel, P.; Trupke, T.; Puzzer, T.; Schäffer, E.; Warta, W. & Glunz, S.W., *Journal of Applied Physics*, AIP, 2007, 101, 123110
- [2] Basore, P., *Conference Record of the Twenty Third IEEE*, 1993, 147-152
- [3] Schöffthaler, M. & Brendel, R., *Journal of Applied Physics*, AIP, 1995, 77, 3162
- [4] Sinton, R.; Cuevas, A.; Stuckings, M.; Consulting, S. & San Jose, C., *Conference Record of the Twenty Fifth IEEE*, 1996, 457-460
- [5] Isenberg, J.; Riepe, S.; Glunz, S. & Warta, W. *Journal of Applied Physics*, AIP, 2003, 93, 4268
- [6] The, M.; Schubert, M.C.; Warta, W., *22nd European Photovoltaic Solar Energy Conference and Exhibition*, 2007
- [7] Trupke, T.; Bardos, R. & Abbott, M., *Applied Physics Letters*, AIP, 2005, 87, 184102
- [8] Würfel, P., *Physics of Solar cells*, Wiley-VCH, 2004
- [9] Würfel, P., *Journal of Physics C: Solid State Physics*, 1982, 15, 3967-3985
- [10] Würfel, P.; Finkbeiner, S. & Daub, E., *Applied Physics A: Materials Science & Processing*, Springer, 1995, 60, 67-70
- [11] correspondence with filter manufacturer, Schott AG, Mainz, Germany
- [12] Hermle, M., PhD-Thesis, to be published, 2008
- [13] Breitenstein, O. & Langenkamp, M., *Lock-In Thermography*, Springer, 2003
- [14] Schubert, M.C., PhD-Thesis, University of Constance, 2008
- [15] The, M., Diploma-Thesis, University of Freiburg, 2007
- [16] Hermle, M.; Schneiderlöchner, E.; Grupp, G. & Glunz, S.W., *20th European Photovoltaic Solar Energy Conference and Exhibition*, 2005
- [17] The, M.; Giesecke, J.; Kasemann, M.; Warta, W.; *23rd European Photovoltaic Solar Energy Conference and Exhibition*, 2008
- [18] Green, M. & Keevers, M., *Progress in Photovoltaics*, 1995, 3, 189-192
- [19] Green, M., *Silicon solar cells: advanced principles & practice*, University of New South Wales, Sydney, NSW, Australia, 1995
- [20] Weakliem, H. & Redfield, D., *Journal of Applied Physics*, AIP, 1979, 50, 1491
- [21] Herzinger, C.; Johs, B.; McGahan, W.; Woollam, J. & Paulson, W., *Journal of Applied Physics*, AIP, 1998, 83, 3323
- [22] Aspnes, D. et al., *Properties of Silicon*, INSPEC (The Institute of Electrical Engineers EMIS Datareview RN, 1988)